

Design of Liquid Crystals with “de Vries-like” Properties: Frustration between SmA- and SmC-Promoting Elements

Jeffrey C. Roberts,[†] Nadia Kapernaum,[‡] Qingxiang Song,[†]
Dorothee Nonnenmacher,[‡] Khurshid Ayub,[†] Frank Giesselmann,[‡] and
Robert P. Lemieux^{*†}

Chemistry Department, Queen’s University, Kingston, Ontario K7L 3N6, Canada, and Institute of Physical Chemistry, Universität Stuttgart, Pfaffenwaldring 55, D-70569 Stuttgart, Germany

Received October 14, 2009; E-mail: lemieux@chem.queensu.ca

Abstract: According to a new design strategy for “de Vries-like” liquid crystal materials, which are characterized by a maximum layer contraction of $\leq 1\%$ upon transition from the SmA phase to the SmC phase, we report the synthesis and characterization of two homologous series of organosiloxane mesogens. The design of these new materials is based on a frustration between one structural element that promotes the formation of a SmC phase (a trisiloxane-terminated side-chain) and one that promotes the formation of a SmA phase (either a chloro-terminated side-chain or a 5-phenylpyrimidine core). Measurements of smectic layer spacing d as a function of temperature by small-angle X-ray scattering (SAXS) combined with optical tilt angle measurements revealed that the mesogens 5-(4-(11-(1,1,1,3,3,5,5-heptamethyltrisiloxanyl)-undecyloxy)phenyl)-2-(1-alkyloxy)pyrimidine (**3(n)**) undergo SmA–SmC phase transitions with maximum layer contractions ranging from 0.5% to 1.4%. A comparison of reduction factors R and f suggests that this behavior is due in part to a pronounced negative thermal expansion in the SmC phase that counterbalances the layer contraction caused by increasing tilt. SAXS measurements also revealed that compounds **3(n)** are characterized by low orientational and high translational order, which is consistent with theoretical predictions that such materials should exhibit de Vries-like properties. The R values for series **3(n)** are comparable to, and even lower than, those reported for established de Vries-like materials such as the perfluorinated 2-phenylpyrimidine material **3M 8422**.

Introduction

The self-organization of amphiphilic molecules forming liquid crystal phases is generally described as the nanosegregation of two or more incompatible segments into distinct domains with topographies dictated by molecular shape and amphiphilic interfacial curvature.¹ The formation of lamellar smectic phases by calamitic (rod-shaped) mesogens is driven by the nanosegregation of rigid aromatic cores from flexible aliphatic side-chains and may be further promoted by the introduction of incompatible segments such as perfluorinated side-chains or oligomeric siloxane end-groups. The fluid smectic A (SmA) and smectic C (SmC) phases have diffuse lamellar structures described by a density wave with a period d corresponding to the smectic layer spacing.² In the uniaxial SmA phase, the axes of orientational and translational order are coincident, with the director n parallel to the smectic layer normal z ; in the biaxial SmC phase, n is tilted relative to z by a tilt angle θ that varies with temperature. According to the classic rigid-rod model shown in Figure 1a, the SmA–SmC phase transition is

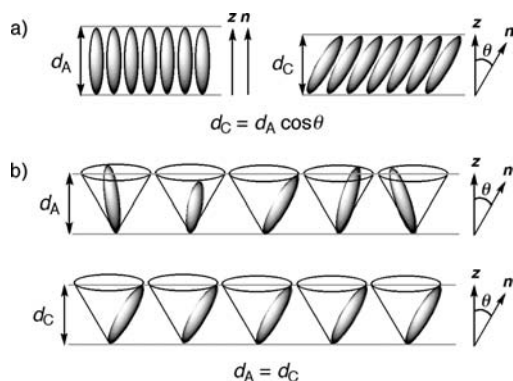


Figure 1. Schematic representations of the SmA–SmC phase transition according to (a) a classic rigid-rod model and (b) the diffuse cone model proposed by de Vries.⁴

accompanied by a contraction of the layer spacing d that scales with the cosine of the tilt angle θ and is typically on the order of 7–10% in conventional calamitic materials.³ This layer contraction has been a problem in the formulation of chiral SmC* mixtures for ferroelectric liquid crystal (FLC) display devices, which may be solved by a design strategy focused on balancing nanosegregation and low orientational order (vide infra).

[†] Queen’s University.

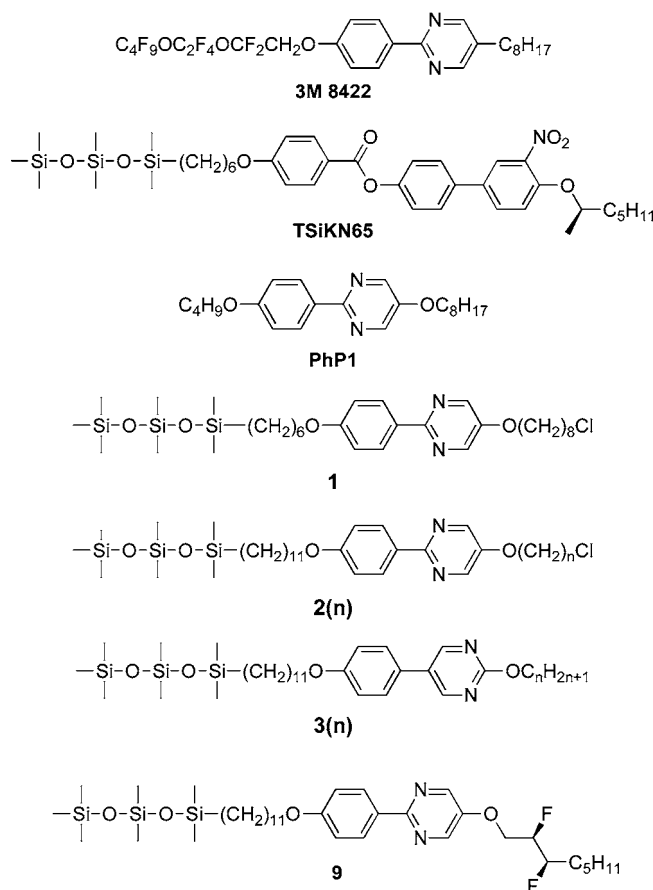
[‡] Universität Stuttgart.

- (1) (a) Tschierske, C. *J. Mater. Chem.* **1998**, *8*, 1485–1508. (b) Goodby, J. W.; Mehl, G. H.; Saez, I. M.; Tuffin, R. P.; Mackenzie, G.; Auzély-Velty, R.; Benvegnu, T.; Plusquellec, D. *Chem. Commun.* **1998**, 2057–2070. (c) Tschierske, C. *J. Mater. Chem.* **2001**, *11*, 2647–2671.
(2) (a) McMillan, W. L. *Phys. Rev. A* **1971**, *4*, 1238–1246. (b) McMillan, W. L. *Phys. Rev. A* **1972**, *6*, 936–947.

- (3) Lagerwall, J. P. F.; Giesselmann, F. *ChemPhysChem* **2006**, *7*, 20–45.

In a surface-stabilized planar alignment, the chiral SmC* phase has ferroelectric properties: it exhibits a spontaneous electric polarization P_S perpendicular to the tilt plane that can be coupled to an electric field to produce an ON–OFF light shutter switching between opposite tilt orientations on a microsecond time scale.^{5,6} Materials used in FLC display applications are normally composed of an achiral liquid crystal mixture and a chiral dopant that induces a spontaneous polarization in the SmC phase. To produce a uniform alignment between parallel rubbed polyimide-coated ITO glass slides, the liquid crystal material is cooled from the isotropic phase to the SmC* phase via the SmA* phase, which normally results in a buckling of the smectic layers into a chevron geometry due to the combined effect of surface anchoring and the layer contraction depicted in Figure 1a. Chevrons of opposite fold directions are separated by zigzag line defects, which severely degrade the optical quality of the FLC film.⁷

One solution to this problem is to develop materials with minimal layer contraction at the SmA–SmC phase transition. Over the past 20 years, several groups have focused on a class of liquid crystal materials referred to as “de Vries-like”, which are characterized by maximum layer contractions of $\leq 1\%$ upon transition from the SmA phase to the SmC phase.^{3,8–14} This reference stems from the diffuse cone model proposed by de Vries that describes the SmA phase as a lamellar structure in which mesogens have a tilted molecular orientation and random azimuthal distribution.⁴ According to this idealized model, the SmA–SmC transition is described as an ordering of the azimuthal distribution that results in zero layer contraction, as shown in Figure 1b. In fact, the structure of the SmA phase formed by de Vries-like materials has yet to be fully elucidated, but recent theoretical studies do suggest that calamitic materials combining low orientational order and high lamellar order are likely to exhibit this behavior.^{15,16} This is consistent with the fact that most de Vries-like materials feature nanosegregating structural elements such as siloxane end-groups or perfluorinated side-chains that strongly promote lamellar ordering.³ Examples of such materials include **3M 8422** and **TSiKN65**, which show maximum layer contractions of 0.4% and 0.65%, respectively.^{10,11}



Although there are now several examples of liquid crystals with de Vries-like properties, there is still no strategy for the rational design of these unusual materials. In an effort to develop de Vries-like liquid crystal hosts that are structurally similar to components of FLC mixtures, we have shown that one can increase the “de Vries character” of **PhP1** by integrating one structural element that promotes the formation of a SmC phase (trisiloxane end-group) with one that promotes the formation of a SmA phase (chloro-terminated side-chain).¹⁷ The “de Vries character” of a liquid crystal material can be expressed by the reduction factors R and f according to eqs 1 and 2:

$$R = \delta(T)/\theta_{\text{opt}}(T) = \cos^{-1}[d_C(T)/d_{AC}]/\theta_{\text{opt}}(T) \quad (1)$$

$$f = \theta_{\text{Xray}}(T)/\theta_{\text{opt}}(T) = \cos^{-1}[d_C(T)/d_A(T)]/\theta_{\text{opt}}(T) \quad (2)$$

In eq 1, $\delta(T)$ is the tilt angle required to give the observed layer contraction relative to the layer spacing at the SmA–SmC transition d_{AC} assuming a rigid-rod model;⁸ in eq 2, $\theta_{\text{Xray}}(T)$ is the tilt angle required to give the observed layer contraction relative to the SmA layer spacing $d_A(T)$ extrapolated in the SmC phase at a given reduced temperature according to a least-squares fit of the data points in the SmA phase near the SmA–SmC transition.¹⁰ The latter gives a reduction factor that is normalized with respect to negative thermal expansion. In each equation, the tilt angle derived from layer spacing measurements is divided by the optical tilt angle $\theta_{\text{opt}}(T)$ measured by polarized optical microscopy (POM).

As shown in Figure 2, the trisiloxane derivatives **1** and **2(8)** undergo SmA–SmC phase transitions with maximum layer contractions of 4.2% and 1.6%, respectively, which are signifi-

- (4) de Vries, A. *J. Chem. Phys.* **1979**, *71*, 25–31.
 (5) Clark, N. A.; Shao, R.; Clark, N. A. *Appl. Phys. Lett.* **1980**, *36*, 899–901.
 (6) Lagerwall, S. T. *Ferroelectric and Antiferroelectric Liquid Crystals*; Wiley–VCH: Weinheim, 1999.
 (7) Rieker, T. P.; Clark, N. A.; Smith, G. S.; Parmar, D. S.; Sirota, E. B.; Safinya, C. R. *Phys. Rev. Lett.* **1987**, *59*, 2658–2661.
 (8) Takanishi, Y.; Ouchi, Y.; Takezoe, H.; Fukuda, A.; Mochizuki, A.; Nakatsuka, M. *Jpn. J. Appl. Phys.* **1990**, *29*, L984–L986.
 (9) Giesselmann, F.; Zugenmaier, P.; Dierking, I.; Lagerwall, S. T.; Stebler, B.; Kaspar, M.; Hamplova, V.; Glogarova, M. *Phys. Rev. E* **1999**, *60*, 598–602.
 (10) Radcliffe, M. D.; Brostrom, M. L.; Epstein, K. A.; Rappaport, A. G.; Thomas, B. N.; Shao, R.; Clark, N. A. *Liq. Cryst.* **1999**, *26*, 789–794.
 (11) Spector, M. S.; Heiney, P. A.; Naciri, J.; Weslowski, B. T.; Holt, D. B.; Shashidhar, R. *Phys. Rev. E* **2000**, *61*, 1579–1584.
 (12) Lagerwall, J. P. F.; Giesselmann, F.; Radcliffe, M. D. *Phys. Rev. E* **2002**, *66*, 031703.
 (13) Panarina, O. E.; Panarin, Y. P.; Vij, J. K.; Spector, M. S.; Shashidhar, R. *Phys. Rev. E* **2003**, *67*, 051709.
 (14) Naciri, J.; Carboni, C.; George, A. K. *Liq. Cryst.* **2003**, *30*, 219–225.
 (15) (a) Gorkunov, M. V.; Osipov, M. A.; Lagerwall, J. P. F.; Giesselmann, F. *Phys. Rev. E* **2007**, *76*, 051706. (b) Gorkunov, M. V.; Giesselmann, F.; Lagerwall, J. P. F.; Sluckin, T. J.; Osipov, M. A. *Phys. Rev. E* **2007**, *75*, 060701.
 (16) (a) Saunders, K.; Hernandez, D.; Pearson, S.; Toner, J. *Phys. Rev. Lett.* **2007**, *98*, 197801. (b) Saunders, K. *Phys. Rev. E* **2008**, *77*, 061708. (c) Saunders, K. *Phys. Rev. E* **2009**, *80*, 011703.

- (17) Li, L.; Jones, C. D.; Magolan, J.; Lemieux, R. P. *J. Mater. Chem.* **2007**, *17*, 2313–2318.

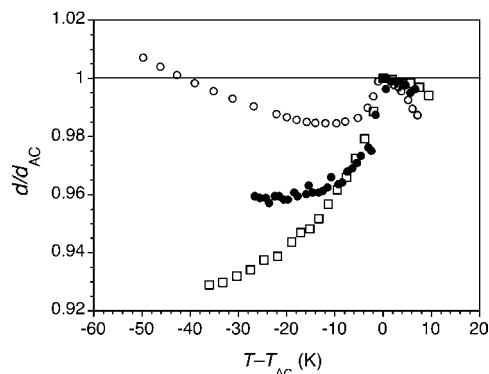


Figure 2. Relative smectic layer spacing d/d_{AC} versus reduced temperature $T - T_{AC}$ for compounds **1** (●), **2(8)** (○), and **PhP1** (□) measured by small-angle X-ray scattering (SAXS).

cantly smaller than the layer contraction of 7.1% observed with **PhP1**.¹⁸ If one takes into account the difference in optical tilt angle θ_{opt} in the SmC phase at a reduced temperature of $T - T_{AC} = -10$ K, the R values for **1** and **2(8)** are 0.57 and 0.43, respectively, again significantly smaller (i.e., more de Vries-like as $R \rightarrow 0$) than the R value of 0.80 measured for **PhP1**. However, these are still far from the R value of 0.18 derived from SAXS measurements reported for **3M 8422**,¹⁰ which is considered to be a benchmark in terms of de Vries character. An interesting feature of the d/d_{AC} versus $T - T_{AC}$ profile of compound **2(8)**, which is also found in the profiles of **3M 8422** and other de Vries-like materials, is the pronounced negative thermal expansion of the layer spacing in the SmA phase that persists in the SmC phase and appears to counterbalance the layer contraction caused by the increasing tilt. This is reflected by a R/f ratio of 0.68 that is much smaller than that of 0.96 for both **1** and **PhP1**. This negative thermal expansion is likely due to an increase in orientational ordering together with an increase in effective molecular length as the alkyl chains become more extended at lower temperature.

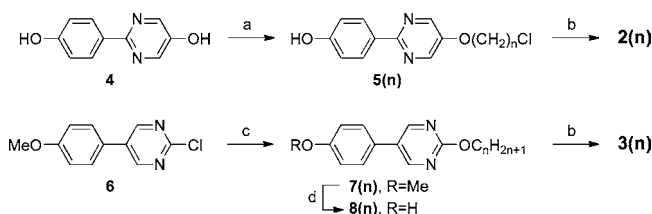
The trisiloxane-terminated undecyloxy side-chain and the chloro-terminated octyloxy side-chain were shown to strongly promote the formation of SmC and SmA phases, respectively.^{17,19} The combination of these two elements, which resulted in the lower R value of compound **2(8)**, may reflect a frustration similar to that invoked in the formation of smectic twist-grain-boundary phases that could form the basis of a rational design strategy for de Vries-like materials.²⁰ To test this hypothesis, and to investigate the effect of broadening the temperature range of the SmA phase on de Vries-like behavior,²¹ we designed a homologous series of trisiloxane mesogens **3(n)** in which the SmA-promoting element is a nonplanar 5-phenylpyrimidine core,²² and we compared their R and f values to those measured for a homologous series of the chloro-terminated trisiloxane

mesogens **2(n)**.²³ These results, together with differential scanning calorimetry, tilt angle, and order parameter measurements, will be discussed in the context of current theoretical models for the SmA–SmC phase transition of de Vries-like liquid crystals.^{15,16}

Results and Discussion

Synthesis. The mesogens **2(n)** were derived from commercially available 2-(4-hydroxyphenyl)-5-pyrimidinol (**4**) via sequential Mitsunobu reactions with the appropriate chloro-terminated alcohols to give **5(n)**, and with 11-(1,1,1,3,3,5,5-heptamethyltrisiloxanyl)-undecanol, as shown in Scheme 1 (see Supporting Information for details). The mesogens **3(n)** were derived from 2-chloro-5-(4-methoxyphenyl)pyrimidine (**6**)²⁴ by a nucleophilic aromatic substitution reaction with the appropriate sodium alkoxides to give **7(n)**, followed by selective demethylation using NaSEt to give **8(n)** and then alkylation via a Mitsunobu reaction with 11-(1,1,1,3,3,5,5-heptamethyltrisiloxanyl)undecanol to give **3(n)**.

Scheme 1^a



^a Reagents and conditions: (a) $\text{HO}(\text{CH}_2)_n\text{Cl}$, DIAD, Ph_3P , THF, 25 °C; (b) $\text{Me}_3\text{SiO}(\text{Me})_2\text{SiO}(\text{Me})_2\text{Si}(\text{CH}_2)_{11}\text{OH}$, DIAD, Ph_3P , THF, 25 °C; (c) $\text{C}_n\text{H}_{2n+1}\text{OH}$, NaH, THF, 25 °C; (d) EtSH, NaH, DMF, reflux.

Mesophase Characterization. The mesophases formed by compounds **2(n)** and **3(n)** were characterized by POM and differential scanning calorimetry (DSC). All compounds in series **2(n)** and **3(n)** form SmA and SmC phases on heating and cooling (Figure 3 and Table S1 in Supporting Information), as shown by the characteristic fan and homeotropic textures of the SmA phase that turn into the broken fan and Schlieren textures of the SmC phase, respectively, with a pronounced change in interference color. The color change of the fan/broken fan texture observed by POM for a 19 μm film of **3(8)** from just above the SmA–SmC transition point to 5 K below is shown in Figure 4. This color change corresponds to an increase in birefringence of ca. 20% based on a Michel–Levy chart, which is comparable to that reported for **3M 8422** and indicates an increase in orientational order that is expected for de Vries-like materials.³ In addition, DSC and POM analyses suggest that compounds **2(4)** and **2(5)** form an unidentified higher order SmX phase below the SmC phase and do not crystallize at temperatures as low as -80 °C.²⁵ As shown in Figure 3, increasing the length of the nonsiloxane side-chain in **2(n)** and **3(n)** results in a gradual decrease of the SmA temperature range (from 36 to 3 K in **2(n)** and from 22 to 1 K in **3(n)**).¹⁸

- (18) Hartley, C. S.; Kapernaum, N.; Roberts, J. C.; Giesselmann, F.; Lemieux, R. P. *J. Mater. Chem.* **2006**, *16*, 2329–2337.
 (19) Goodby, J. W.; Saez, I. M.; Cowling, S. J.; Görtz, V.; Draper, M.; Hall, A. W.; Sia, S.; Cosquer, G.; Lee, S.-E.; Raynes, E. P. *Angew. Chem., Int. Ed.* **2008**, *47*, 2754–2787.
 (20) Kamien, R. D.; Selinger, J. V. *J. Phys.: Condens. Matter* **2001**, *13*, R1–R22.
 (21) The SmA*–C* layer contraction in a homologous series of chiral mesogens was shown to decrease with increasing temperature range of the SmA* phase: Bezner, S.; Krueger, M.; Hamplova, V.; Glogarova, M.; Giesselmann, F. *J. Chem. Phys.* **2007**, *126*, 054902.
 (22) The 5-phenylpyrimidine analogue of **PhP1** only forms a SmA phase (Cr 84 SmA 117 I): Hegmann, T.; Meadows, M. R.; Wand, M. D.; Lemieux, R. P. *J. Mater. Chem.* **2004**, *14*, 185–190.

(23) For a preliminary communication, see: Roberts, J. C.; Kapernaum, N.; Giesselmann, F.; Lemieux, R. P. *J. Am. Chem. Soc.* **2008**, *130*, 13842–13843.

(24) Brown, D. J.; Lee, T.-C. *J. Chem. Soc. C* **1970**, 214–219.

(25) The assignment of a SmX phase is based on the relatively low enthalpy of the SmX–SmC transitions for **2(4)** and **2(5)** (11–15 kJ/mol) as compared to those of the Cr–SmC transitions for the higher homologues (37–53 kJ/mol), and the observation of recrystallization exotherms on heating the higher homologues before the Cr–SmC transitions.

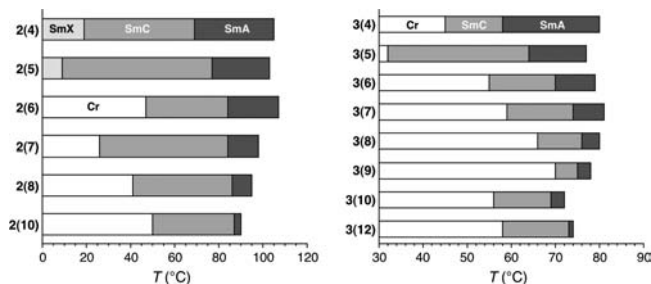


Figure 3. Phase transition temperatures for $2(n)$ and $3(n)$ measured by DSC on heating.

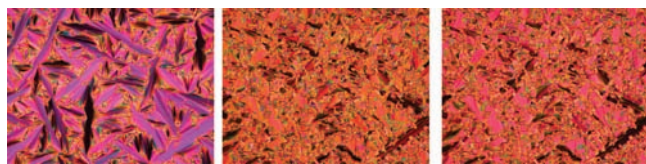


Figure 4. Polarized photomicrographs (100 \times) of compound $3(8)$ in a parallel rubbed glass cell with a spacing of 19 μm at (from left to right) 76, 74, and 70 $^{\circ}\text{C}$. The change in interference color from 76 to 70 $^{\circ}\text{C}$ corresponds to an increase in birefringence of ca. 20%.

Furthermore, the Cr/SmX–SmC transition point shows the expected odd–even effect in $2(n)$ but not in $3(n)$, which shows a gradual increase in the Cr–SmC transition point from $n = 5$ to $n = 9$. The liquid crystal temperature ranges are generally broader in series $2(n)$ than in $3(n)$, and the two shortest homologues in series $2(n)$ are mesogenic in the SmC phase at room temperature.

The DSC analysis suggests that lengthening the alkoxy side-chain causes a change in the nature of the SmA–SmC phase transition of $2(n)$ and $3(n)$. As shown in Figure 5, the increase in enthalpy change for the SmA–SmC phase transition of $3(n)$ (ΔH_{AC}) with increasing alkoxy chain length, from <0.1 to 1.6–1.7 kJ/mol, and the hysteresis of the peak temperatures on heating and cooling for the higher homologues suggest a crossover from a second-order or tricritical SmA–SmC transition at relatively short chain lengths ($n \leq 6$) to a first-order transition at longer chain lengths.²⁶ This trend is consistent with previous observations in homologous series of a second-order SmA–SmC transition becoming discontinuous with decreasing temperature range of the SmA phase.^{27–30} On the other hand, the SmA–SmC phase transition in series $2(n)$ is undetectable by DSC except for the highest homologue $2(10)$, which suggests that the crossover to a first-order transition occurs further down the series, between $n = 8$ and $n = 10$.

Optical Tilt Measurements. Optical tilt angles (θ_{opt}) in the SmC phase were measured as a function of temperature by POM by applying a field of 10 V across surface-stabilized FLC films (5 μm) in ITO glass cells with rubbed Nylon alignment layers using liquid crystal samples doped with the chiral additive **9** (1–2 mol %).³¹ In both series $2(n)$ and $3(n)$, the optical tilt

angle increases with the length of the nonsiloxane side-chain, which is consistent with normally observed trends;¹⁸ at $T - T_{\text{AC}} = -10$ K, θ_{opt} increases from 15 $^{\circ}$ to 25 $^{\circ}$ for $2(n)$, and from 24 $^{\circ}$ to 43 $^{\circ}$ for $3(n)$ (see Table S2 and Figure S1 in Supporting Information). Because the tilt angle is the primary order parameter describing the SmA–SmC phase transition, the temperature variation of θ is described by the power law:

$$\theta \propto |T - T_c|^\beta \quad (3)$$

where β is the order parameter exponent related to the nature of the phase transition and T_c is the phase transition temperature of a theoretical second-order phase transition (critical temperature).³² According to the generalized mean-field theory of phase transitions (Landau theory), a β value of 0.5 is expected in the case of a pure second-order transition, whereas a β value of 0.25 is expected in the case of a SmA–SmC transition at the crossover (tricritical) point from second- to first-order transition.^{33,34} The plots of θ_{opt} versus $|T - T_c|$ for $3(4)$, $3(7)$, and $3(10)$ are compared to the best fits to eq 3 in Figure 6.³⁵ These fits give β values of 0.28, 0.12, and 0.08, respectively, which are consistent with the trend observed in the ΔH_{AC} measurements and suggest a change in the nature of the SmA–SmC transition from tricritical to first-order at $n = 7$. The corresponding fits to eq 3 for $2(4)$, $2(7)$, and $2(10)$ give β values of 0.21, 0.22, and 0.14, respectively, which are also consistent with the ΔH_{AC} measurements and suggest that the SmA–SmC phase transition in this series is tricritical up to $n = 8$ and changes to a first-order transition at $n = 10$.

Reduction Factor Measurements. Accurate measurements of smectic layer spacings (d) as a function of temperature were carried out by small-angle X-ray scattering (SAXS). As shown in Figure 7, the d/d_{AC} versus $T - T_{\text{AC}}$ profiles for series $2(n)$ are qualitatively similar and show a negative thermal expansion in the SmA phase that persists in the SmC phase to such an extent that the layer spacing in the SmC phase (d_c) exceeds the spacing at the SmA–SmC transition (d_{AC}) at reduced temperatures as high as -20 K. The maximum layer contraction increases with the length of the chloroalkoxy side-chain, from 0.5% for $2(4)$ to 1.5% for $2(10)$, which correlates with the increase in θ_{opt} . The d/d_{AC} versus $T - T_{\text{AC}}$ profiles for series $3(n)$ also show a negative thermal expansion in both the SmA and the SmC phases. However, these profiles show two separate trends with a break that may correspond to the apparent change in SmA–SmC transition from tricritical to first-order. As shown in Figure 7, the profiles for the lower homologues $3(4)$ to $3(6)$ are very similar and show a maximum layer contraction of 0.5%, which jumps to 1.4% with $3(7)$ and then progressively decreases with increasing alkoxy chain length to 0.5% with $3(10)$. The SmA temperature range of $3(12)$ is too narrow to detect any layer contraction, and the profile only shows d_c increasing due to the negative thermal expansion.

(26) Thoen, J. In *Physical Properties of Liquid Crystals*; Demus, D., Goodby, J. W., Gray, G. W., Spiess, H.-W., Vill, V., Eds.; Wiley-VCH: Weinheim, 1999; pp 208–232.

(27) Huang, C. C.; Lien, S. C. *Phys. Rev. E* **1985**, *31*, 2621–2627.

(28) Ratna, B. R.; Shashidhar, R.; Nair, G. G.; Prasad, S. K.; Bahr, C.; Heppke, G. *Phys. Rev. A* **1988**, *37*, 1824–1826.

(29) Prasad, S. K.; Raja, V. N.; Shankar Rao, D. S.; Nair, G. G.; Neubert, M. E. *Phys. Rev. A* **1990**, *42*, 2479–2481.

(30) Heinrich, B.; Guillon, D. *Mol. Cryst. Liq. Cryst.* **1995**, *268*, 21–43.

(31) Roberts, J. C.; Kapernaum, N.; Giesselmann, F.; Wand, M. D.; Lemieux, R. P. *J. Mater. Chem.* **2008**, *18*, 5301–5306.

(32) Chandrasekhar, S. *Liquid Crystals*, 2nd ed.; Cambridge University Press: Cambridge, 1992.

(33) Birgeneau, R. J.; Garland, C. W.; Kortan, A. R.; Litster, J. D.; Meichle, M.; Ocko, B. M.; Rosenblatt, C.; Yu, L. J.; Goodby, J. *Phys. Rev. A* **1983**, *27*, 1251–1254.

(34) Landau, L. D. *Statistical Physics*, 3rd ed.; Pergamon Press: Oxford, 1980.

(35) Because of the relatively low temperature resolution in the optical tilt angle measurements (± 0.5 K), a precise value of the critical temperature T_c cannot be obtained; $T_{\text{AC}} < T_c$ for a first-order transition, whereas $T_{\text{AC}} = T_c$ for a second-order transition. The fits to eq 3 over the full temperature range of the SmC phase are primarily intended to confirm the trends in ΔH_{AC} observed by DSC.

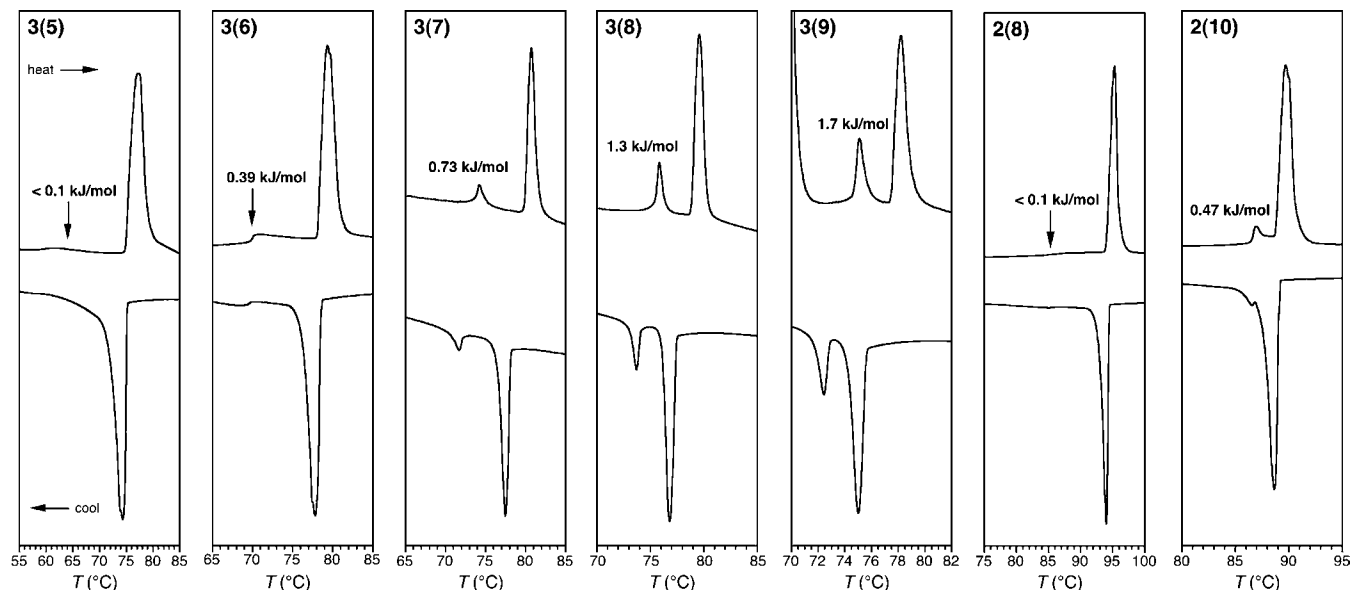


Figure 5. Partial DSC traces of compounds **3(5)–3(9)**, **2(8)**, and **2(10)** showing the SmC–SmA and SmA–I phase transitions on heating and cooling at 5 K/min, and the enthalpy change for the SmA–SmC phase transition ΔH_{AC} in kJ/mol.

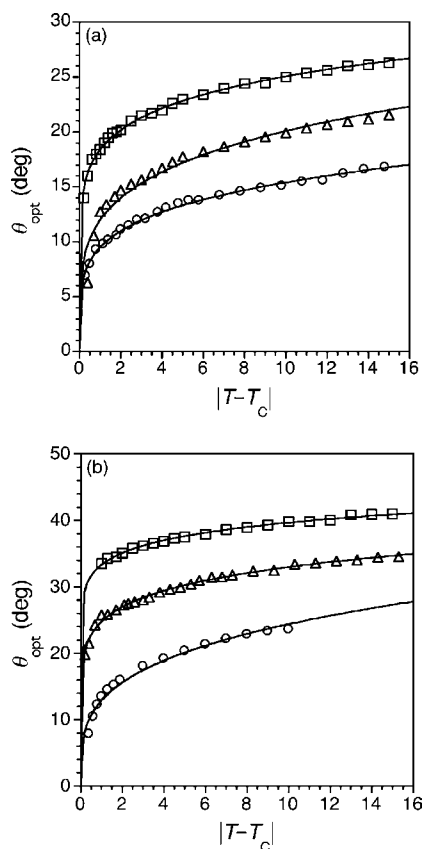


Figure 6. Optical tilt angles θ_{opt} versus reduced temperature $T - T_c$ for (a) compounds **2(4)** (○), **2(7)** (△), and **2(10)** (□), and (b) compounds **3(4)** (○), **3(7)** (△), and **3(10)** (□). The solid lines represent the fits to eq 3.

Although the maximum layer contractions measured for compounds **2(n)** and **3(n)** upon SmA–SmC phase transition are in the same range, the R values for **3(n)** are significantly smaller than those for **2(n)** because of the difference in optical tilt angles (eq 1). As shown in Figure 8, the R values in series **2(n)** range from 0.36 to 0.47 at $T - T_{AC} = -10$ K, whereas the R values in series **3(n)** range from 0 to 0.30; in the case of

3(10), the layer spacing d_{AC} is restored at $T - T_{AC} = -10$ K due to the negative thermal expansion, within ± 0.1 Å.

To assess the contribution of negative thermal expansion in offsetting the layer contraction due to increasing tilt, the f factors were calculated for **2(n)** and **3(n)** (eq 2). The negative thermal expansion of the layer spacing d in the SmA phase is due primarily to an increase in orientational ordering according to eq 4, where L corresponds to the molecular length l , assuming a monolayer structure, and S_2 is the orientational order parameter (vide infra).^{3,36} The latter can be expressed by a power law function (eq 5), according to the general theory of phase transitions and critical phenomena, where T^* is the superheating limit in K ($T^* > T_1$) and $1 - \alpha$ is the power law exponent ($\alpha \leq 1$).³⁷ Hence, the layer spacing in the SmA phase can be expressed as a function of T according to eq 6:

$$d_A = L/3(S_2 + 2) \quad (4)$$

$$S_2 = (1 - T/T^*)^{1-\alpha} \quad (5)$$

$$d_A = L/3[(1 - T/T^*)^{1-\alpha} + 2] \quad (6)$$

For materials that exhibit only a small negative thermal expansion in the SmA phase, the power law exponent α converges toward zero. In their original calculation of f for **3M 8422**, Ratcliffe et al. assumed that $\alpha = 0$ near the SmA–SmC phase transition and extrapolated d_A into the SmC phase according to a least-squares fit of the data points at $T - T_{AC} \geq 0$.¹⁰ In the present case, the f factors were calculated for **2(n)** and **3(n)** by fitting the data points in Figure 7 at $T - T_{AC} \geq 0$ to eq 6 and extrapolating d_A according to these fits into the SmC phase at $T - T_{AC} = -10$ K (see Figure 9, for example, and Figure S2 in Supporting Information). As shown in Figure 10, the f factors of all compounds in series **2(n)** and **3(n)** are larger than the corresponding R factors. This suggests that negative

(36) In the case of organosiloxane mesogens, which form partially bilayered smectic phases, $l < L < 2l$: Ibn-Elhaj, M.; Skoulios, A.; Guillon, D.; Newton, J.; Hodge, P.; Coles, H. J. *J. Phys. II France* **1996**, *6*, 271–279.

(37) Stanley, H. E. *Introduction to Phase Transitions and Critical Phenomena*; Oxford University Press: Oxford, 1971.

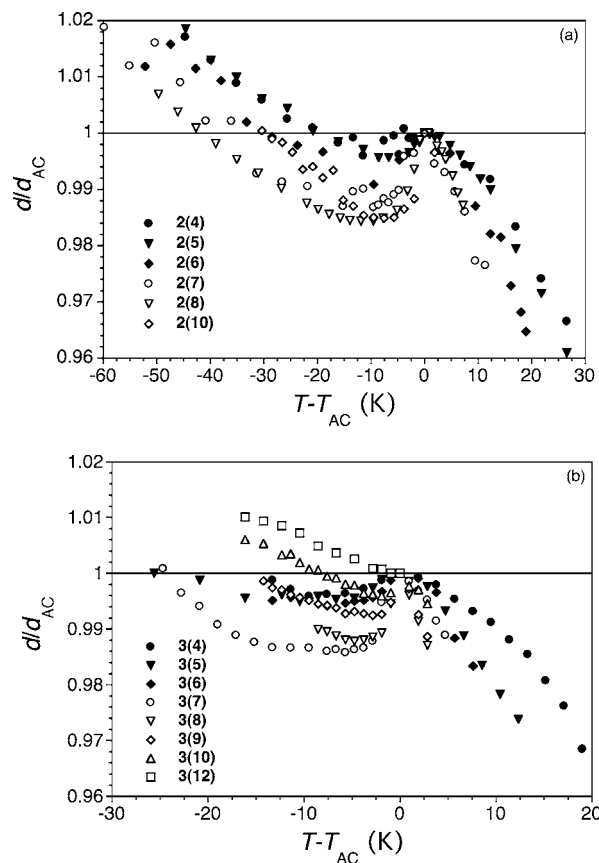


Figure 7. Relative smectic layer spacing d/d_{AC} versus reduced temperature $T - T_{AC}$ for (a) compounds $2(n)$ and (b) compounds $3(n)$. The measurements were performed on heating from the crystalline phase for all compounds except $3(9)$ and $3(10)$, which were performed on cooling from just below the clearing point due to the narrow SmC temperature ranges. The data for $2(8)$ are from ref 17.

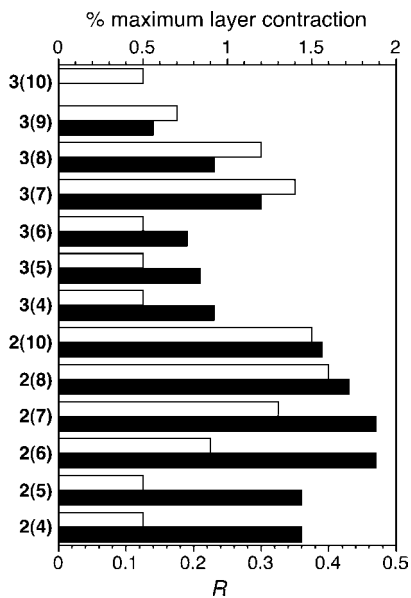


Figure 8. Bar graphs showing reduction factors R at $T - T_{AC} = -10$ K (■) and maximum layer contractions (□) for compounds $2(n)$ and $3(n)$.

thermal expansion in the SmC phase does counterbalance to some extent the layer contraction caused by increasing tilt and results in enhanced de Vries-like properties relative to the parent compound **PhP1**, which shows little negative thermal expansion

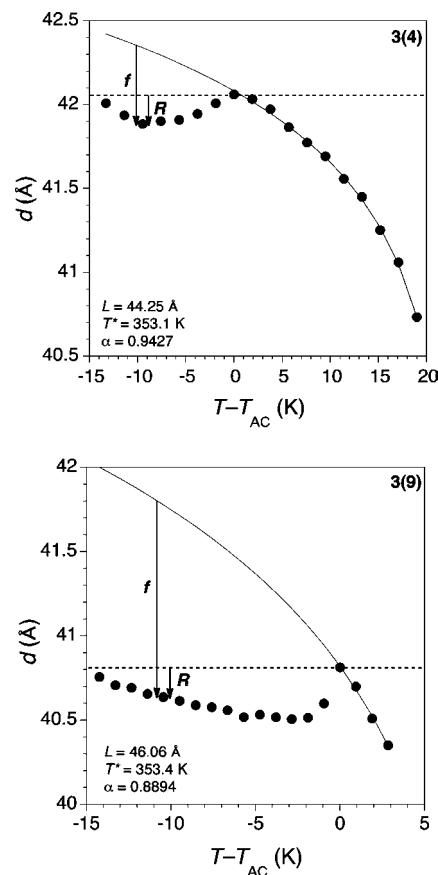


Figure 9. Smectic layer spacing d versus reduced temperature $T - T_{AC}$ for compounds $3(4)$ and $3(9)$. The dashed lines show the layer spacing at the SmA-SmC transition. The solid lines represent the fits to eq 6 for the data points at $T - T_{AC} \geq 0$. The arrows indicate the difference in layer spacing for calculating the R and f reduction factors.

and lies near the solid line corresponding to $R = f$. More significantly, the points corresponding to compounds $3(n)$ are clustered around that corresponding to **3M 8422**, except for compound $3(10)$, which shows no layer contraction at $T - T_{AC} = -10$ K.

Order Parameter Measurements. Recent theoretical models by Osipov and Saunders support the experimental evidence³ that smectogenic materials combining low orientational and high translational order are likely to exhibit de Vries-like properties.^{15,16} To test this prediction, orientational (S_2) and translational (Σ) order parameters were measured in the SmA phase as a function of temperature for the representative compounds $2(8)$, $3(5)$, and **PhP1**. The order parameter S_2 is a measure of the long-range orientational ordering of long molecular axes relative to the director n . In the nematic or smectic A phases, it is derived experimentally from the intensity profile $I(\chi)$ around the wide-angle arc of diffuse X-ray scattering.^{38,39} The order parameter Σ is a measure of the one-dimensional translational ordering (i.e., lamellar ordering) in the SmA phase.² It is defined as the amplitude of the density wave arising from the 1D-periodic smectic layer structure; Σ was determined experimentally by a method previously described by Kapernaum and Giesselmann.⁴⁰ As shown in Figure 11, both organosiloxanes $2(8)$ and $3(5)$ exhibit unusually low orientational order in the SmA phase, with S_2 values in the range of 0.45, as compared to the conventional parent compound **PhP1** with a S_2 value of ca. 0.65. The translational order of both $3(5)$ and **PhP1** is very

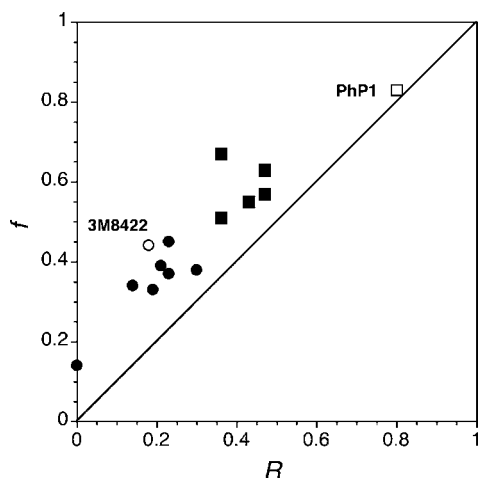


Figure 10. Plot of R versus f for compounds $2(n)$ (■), $3(n)$ (●), PhP1 (□), and 3M 8422 (○) at $T - T_{AC} = -10$ K.

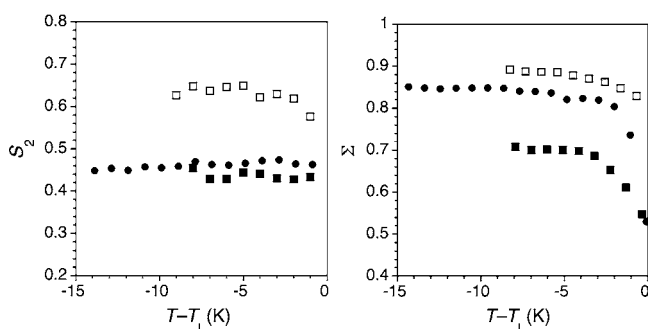


Figure 11. Plots of order parameters S_2 and Σ versus reduced temperature $T - T_1$ (T_1 is the SmA–isotropic transition temperature) for compounds $2(8)$ (■), $3(5)$ (●), PhP1 (□).

high, which is somewhat unexpected in the case of PhP1 considering that it lacks a nanosegregating siloxane-end group. On the other hand, the chloro-terminated organosiloxane $2(8)$ exhibits a much lower translational order than $3(5)$, which is consistent with the higher R values of series $2(n)$. Of the three representative compounds, only $3(5)$ combines low orientational and high translational order, which may explain why the R values for series $3(n)$ are comparable to, and even lower than, those reported for established de Vries-like materials such as 3 M 8422

according to the theoretical predictions of Osipov and Saunders.^{15,16}

Conclusions

In comparison to the parent compound PhP1, the reduction factors measured for series $2(n)$ and $3(n)$ support our hypothesis that combining structural elements promoting the formation of SmA and SmC phases in the same molecules causes a frustration that enhances de Vries-like properties. A comparison of R and f factors suggests that such enhancement may be due in part to a pronounced negative thermal expansion in the SmC phase that counterbalances the layer contraction caused by increasing tilt. Although enhancement in de Vries-like properties is observed in both series, only compounds in series $3(n)$ may be considered “de Vries-like” with properties comparable to that of 3M 8422. This is consistent with the finding that, of the three representative compounds for which order parameters were measured, only $3(5)$ shows a combination of low S_2 and high Σ , which is in agreement with theoretical predictions made by Osipov and Saunders.^{15,16} According to the generalized mean-field theory developed by Saunders, the SmA–SmC phase transition of materials with low orientational and high translational order should be either second-order near the tricritical point or first-order, which is consistent with the DSC and optical tilt angle results obtained for $2(n)$ and $3(n)$.¹⁶ From a practical point of view, materials such as $3(5)$, which forms a SmC phase near room temperature and has a saturated tilt of $\sim 27^\circ$, may be useful as a component of FLC formulations with bookshelf geometry.

Acknowledgment. We are grateful to the Natural Sciences and Engineering Research Council of Canada (NSERC), the Canada Foundation for Innovation, and the Deutsche Forschungsgemeinschaft (DFG) for support of this work.

Supporting Information Available: Syntheses of compounds $2(n)$ and $3(n)$, tables of phase transition temperatures and enthalpies of transition, layer spacings and reduction factors, and plots of θ_{opt} versus $T - T_{AC}$ and d/d_{AC} versus $T - T_{AC}$. This material is available free of charge via the Internet at <http://pubs.acs.org>.

JA9087727

- (38) Davidson, P.; Petermann, D.; Levelut, A.-M. *J. Phys. II France* **1995**, *5*, 113–131.
 (39) Giesselmann, F.; Germer, R.; Saipa, A. *J. Chem. Phys.* **2005**, *123*, 034906.
 (40) Kapernaum, N.; Giesselmann, F. *Phys. Rev. E* **2008**, *78*, 062701.